IEEE Access
Multidisciplinary | Rapid Review | Open Access Journal

Received November 9, 2019, accepted November 22, 2019, date of publication November 26, 2019,
date of current version December 13, 2019.

Digital Object Identifier 10.1109/ACCESS.2019.2955985

A New Active Control Strategy for Pantograph in High-Speed Electrified Railways Based on Multi-Objective Robust Control

JING ZHANG, HANTAO ZHANG, BAOLIN SONG, SONGLIN XIE, AND ZHIGANG LIU, (Senior Member, IEEE)
School of Electrical Engineering, Southwest Jiaotong University, Chengdu 610031, China
Corresponding author: Jing Zhang (sdzj2006@126.com)

This work was supported in part by the National Nature Science Foundation of China (U1734202).

ABSTRACT In high-speed railways, the quality of current collection of high-speed train is directly determined by the contact force between the contact wire of the catenary and the registration strip of the pantograph. In order to ensure a stable contact force, this paper proposes a control strategy for active pantographs by minimizing the acceleration of pantograph collector. The model of pantograph-catenary interaction is established based on the finite element approach and the multibody dynamics. A Kalman filter is designed to obtain the states of the pantograph considering complex electromagnetic circumstances and severe physical environments. According to the equation of motion for the pantograph-catenary system, the implicit expression of pantograph-catenary contact forces is derived. The factors causing the fluctuation of the contact force are analyzed to determine the three control targets, which are minimize the acceleration of pantograph collector, limit the control force and displacement constraint. At last, a multi-objective robust control method based on state estimation is designed. The robustness and effectiveness of the control method are verified on a nonlinear pantograph-catenary system model under different work conditions. The results show that the error between the estimated value and the true value of the pantograph is between 0.06% and 3.46%. The standard deviation of contact force is reduced by 29.55%, 25.26%, and 20.86% under different operational speeds, respectively. The standard deviation of the contact force was still reduced considering the parameter perturbation of pantograph and the unevenness of contact lines. The result of proposed control strategy is better than previous work, even though the proposed controller requires a lower energy consumption. In addition, With the proper pre-treatment of the active control force, the movement number of the actuator is reduced and the control performance is still fine.

INDEX TERMS High-speed pantograph, state estimation, Kalman filter, multi-objective robust control, pantograph-catenary contact force.

I. INTRODUCTION

In recent years, the high-speed railway technologies have been receiving great attention. An important factor affecting the safe and reliable operation of high-speed railway is the quality of current collection of the pantograph-catenary system (PCS) [1], which is directly reflected by the fluctuation of the pantograph-catenary contact force (PCCF) as show in Fig. 1(a). The pantograph-catenary contact force [2] fluctuation may result in the occurrence of arcing and extra wear of registration strips as well as other security problems as show in Fig. 1(b). In fact, the fluctuation of the contact force is mainly affected by the increasing speed of the train and the environmental perturbations, which brings more challenges to a better current collection quality. This paper attempts to make a contribution to this topic.

In order to reduce the fluctuation of contact force, the coupling dynamics of the pantograph-catenary has been deeply studied. An optimization approach for the pantograph suspension system was proposed to ensure a stable current collection quality [3]–[5]. However, these measures have limited potentials in improving the dynamic performance, not exceeding 10%–15% on the decrease of the standard deviation of the contact force. Similarly, lots of works have been carried

The associate editor coordinating the review of this manuscript and approving it for publication was Ruilong Deng.

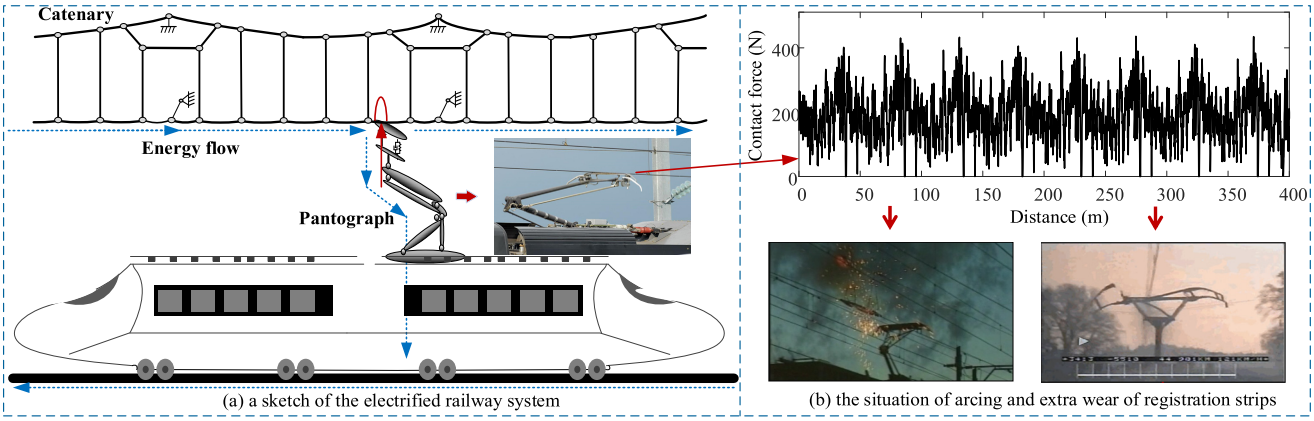

FIGURE 1. The electrified railway system and its some problem.

out on catenary parameter optimization [6], [7] to improve its wind-resistance capability [8], [9] and wave propagation behaviour [10]. However, the parameter optimization cost is huge, and it is difficult to implement due to the tension limit and the material limit. Apart from the structural optimization, the active control technique for the pantograph is another way to improve the current collection quality of pantograph-catenary system, which has good potential to reduce the fluctuation of contact force, and has great adaptability to different types of catenary, but there are still some issues that deserve further attention.

First of all, the primary issue is to design a high-efficiency controller. The previous studies on this topic mainly focused on control strategies. The most widely used method was proportional-integral-derivative (PID) control [11]–[13], and others included fuzzy control [14], sliding mode control [15], [16], optimal control [17], [18], and so on. In these controllers, the contact force was mainly used as the feedback. Currently, the contact fore is calculated by the acceleration of the pantograph strip, the inertia force and the aerodynamic forces, which definitely brings some errors to estimate the contact force. In this paper, the acceleration of the pantograph strip is directly used as the feedback. The dramatic change in the acceleration is able to represent the sharp fluctuation of PCCF, which is explained in the third section.

The second issue is regarding the acquisition of the pantograph states, which are used as the feedback in the active pantograph. Most previous works [16]–[20] adopted the state information of the PCS, in their controllers, but the acquisition of the state information was not reported, the complexity of the PCS environment can easily lead to measurement errors. State estimation is a suitable method to eliminate the errors. It has been used reliably in various engineering backgrounds [21]. In order to reduce the negative effect of the severe electromagnetic interference and environment perturbations, a Modified Kalman filter (MKF) [22] is adopted to obtain the pantograph states in PCS. It has the corresponding advantage to overcome the adverse effects caused by the inherent error of the model during the state estimation process.

The last issue is the validation of the proposed control strategy with a nonlinear PCS model. Compared with most of the existing oversimplified linear models, the nonlinear PCS model is more realistic and complicated, which may cause the failure of the controller. So, it is necessary to verify with a nonlinear PCS model [16]–[18], [23]. Among them, the pantograph is normally established by a two or three-level mass-spring-damper systems and the catenary is established based on nonlinear cable and truss elements [24]–[25]. In addition, the uncertainty of the material and structural parameters may lead to the mismatch of the numerical model with respective to its realistic conditions, whose effect on the control performance is also investigated.

According to the above discussion, most active pantograph control strategy uses a feedback control system. In addition, most of these control strategies produce high-frequency control force that puts higher demands on actuator configuration. Addressing this matter, this paper proposes a new control strategy to reduce the fluctuation of PCCF by minimizing the acceleration of pantograph collector (PCA), which is verified with a nonlinear PCS model. Compared with previous controller, the result of proposed control strategy is better than previous work, even though the proposed controller requires a lower energy consumption. In addition, With the proper pre-treatment of the active control force, the movement number of the actuator is reduced, which can reduce the negative effects of time delay, and the control is still effective.

The main contents of this study and their relationship are shown in Fig. 2. The finite element model of catenary is established and validated in section II. According to the coupled equation of motion for PCS, a multi-objective robust control method based on the state estimation is proposed in Section III. Section IV verifies the effectiveness and stability of the controller. Finally, the research conclusions of this paper are summarized.

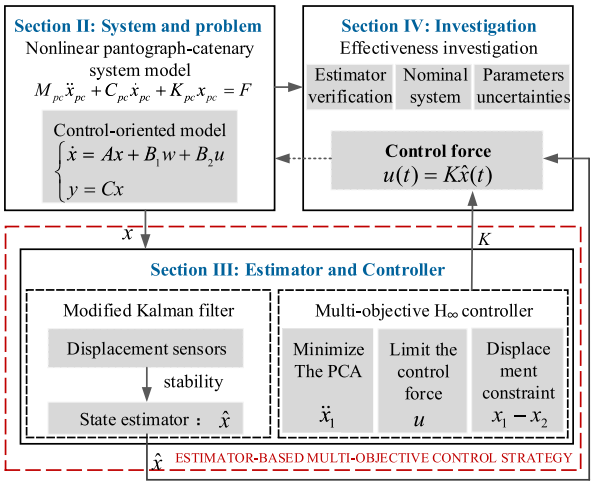

FIGURE 2. Main contents and their relations in this study.

II. PANTOGRAPH-CATENARY MODEL

A. PANTOGRAPH MODEL

The lumped-mass model is an efficient approach to describe the behaviours of the pantograph [24], [25]. In this paper, the three-degree-of-freedom lumped model of pantograph is adopted, which is a good representative of the physical characteristics of the real pantograph. The specific structure is shown in Fig. 3. Based on multibody dynamics, the equation of motion for the pantograph is obtained.

$$\begin{cases} m_1\ddot{x}_1+c_1(\dot{x}_1-\dot{x}_2)+k_1(x_1-x_2)=F_{pc} \\ m_2\ddot{x}_2+c_1(\dot{x}_2-\dot{x}_1)+c_2(\dot{x}_2-\dot{x}_3) \\ +k_1(x_2-x_1)+k_2(x_2-x_3)=0 \\ m_3\ddot{x}_3+c_2(\dot{x}_3-\dot{x}_2)+c_3\dot{x}_3+k_2(x_3-x_2) \\ +k_3x_3=F_l+u(t) \end{cases} \tag{1}$$

where, m_1, m_2 and m_3 are the mass of the collector, upper, and lower frames of a pantograph, respectively. k_1, k_2, k_3 and c_1, c_2, c_3 represent the stiffness and damping of the collector, upper frame and lower frame, respectively. x_1, x_2, x_3 denote the vertical displacement of each mass, F_{pc} is the contact force, F_l is the static lift force, and u is the control force.

Defining the state variables as $\mathbf{x}_p=[x_1,x_2,x_3]^T$, Eq. (1) can be simplified as

$$\mathbf{M}_p\ddot{\mathbf{x}}_p+\mathbf{C}_p\dot{\mathbf{x}}_p+\mathbf{K}_p\mathbf{x}_p=\mathbf{F}_p \tag{2}$$

where $\mathbf{M}_p=diag\,[m_1,m_2,m_3]$, $\mathbf{F}_p=\left[F_{pc},\ 0,\ u\right]^T$, $\mathbf{C}_p=\begin{bmatrix} c_1 & -c_1 & 0 \\ -c_1 & c_1+c_2 & -c_2 \\ 0 & -c_2 & c_2+c_3 \end{bmatrix}$, $\mathbf{K}_p=\begin{bmatrix} k_1 & -k_1 & 0 \\ -k_1 & k_1+k_2 & -k_2 \\ 0 & -k_2 & k_2+k_3 \end{bmatrix}$.

B. CATENARY MODEL

The catenary is an important part of the electrified railway, and transmits electric power to the high-speed train. It consists of contact wire, droppers, messenger wire, steady arms, etc. The finite element model (FEM) of the catenary is shown in Fig. 4(a) and 4(b). The nonlinear cable element is used

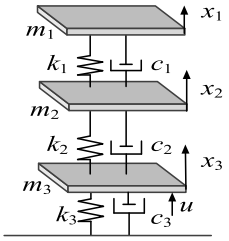

FIGURE 3. Lumped-mass model of pantograph.

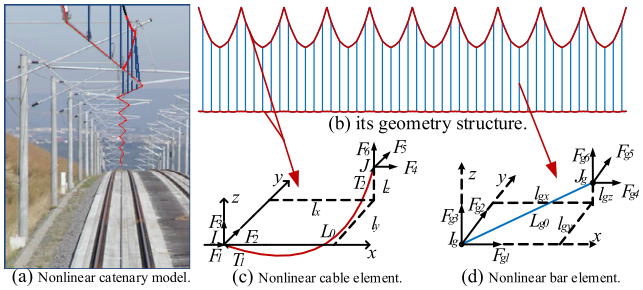

FIGURE 4. (a) FEM catenary model; (b) Nonlinear cable element; (c) Nonlinear bar element.

to model the contact wire and messenger wire as shown in Fig. 4(c). The model of dropper is established based on the nonlinear truss element as shows in Fig. 4(d). The equation of motion for the catenary can be expressed as

$$\mathbf{M}_c\ddot{\mathbf{x}}_c+\mathbf{C}_c\dot{\mathbf{x}}_c+\mathbf{K}_c\mathbf{x}_c=\mathbf{F}_c \tag{3}$$

where $\ddot{\mathbf{x}}_c$, $\dot{\mathbf{x}}_c$ and $\mathbf{x}_c$ denote acceleration, velocity, and displacement of the catenary, respectively. $\mathbf{F}_c$ represents an external force vector acting on the catenary, $\mathbf{M}_c$, $\mathbf{C}_c$, and $\mathbf{K}_c$ respectively represent the mass, damping, and stiffness matrices of the catenary.

Combining (2) and (3) together, the coupled equation of motion for the PCS can be expressed as follows.

$$\mathbf{M}_{pc}\ddot{\mathbf{x}}_{pc}+\mathbf{C}_{pc}\dot{\mathbf{x}}_{pc}+\mathbf{K}_{pc}\mathbf{x}_{pc}=\mathbf{F} \tag{4}$$

where $\mathbf{M}_{pc}=diag\left(\mathbf{M}_c,\mathbf{M}_p\right)$, $\mathbf{C}_{pc}=diag\left(\mathbf{C}_c,\ \mathbf{C}_p\right)$, $\mathbf{x}_{pc}=[\mathbf{x}_c,\mathbf{x}_p]$, $\mathbf{K}_{pc}=diag(\mathbf{K}_c,\mathbf{K}_p)$. '$diag(\ldots)$' denotes a block diagonal matrix.

In order to verify the established pantograph-catenary coupling model, the simulation is performed using the reference model specified in EN 50318, and the results are standardized according to the acceptance range of the standard. The conversion function is as follows

$$y^*=\frac{y-y_{c\_\min}}{y_{c\_\max}-y_{c\_\min}} \tag{5}$$

where $y_{c\_\max}$ and $y_{c\_\min}$ denote upper and lower limits of the standard range, y denotes the simulation results. The results are shown in Fig. 5, which 'st.' means 'statistic'; 'ac.' means 'actual'. It can be seen that all the normalized values fall in (0,1), which means that the present model satisfies the requirement of EN 50318.

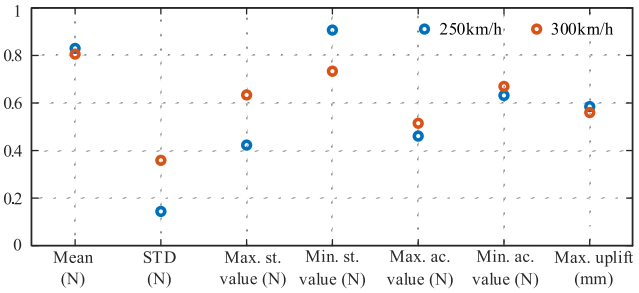

FIGURE 5. Model verification with EN 50318.

III. ESTIMATOR-BASED MULTI-OBJECTIVE COLLECTOR

The control system of pantograph is designed in Fig. 6. A multi-objective robust control strategy based on state estimation is proposed. The former is used to estimate pantograph status information, and the latter is used to reduce the contact force fluctuation.

A. PROBLEM FORMULATION

In previous control strategies, the contact force information was usually measured to reduce the fluctuation of contact force. In this paper, the acceleration of collector is used instead of the contact force as feedback information. Firstly, the factors affecting the fluctuation of contact force are analyzed from the equation of motion. According to (1), the PCCF can be evaluated by

$$F_{pc} = -[m_1\ddot{x}_1 + c_1(\dot{x}_1 - \dot{x}_2) + k_1(x_1 - x_2)] \tag{6}$$

It can be seen from (6) that the value of the PCCF is completely represented by its physical parameters (Table 1) and the state information of pantograph. Moreover, c_1 and $\dot{x}_1 - \dot{x}_2$ are very small, so the expression of the contact force

TABLE 1. Physical parameters of DS380 pantograph.

Parameter	Nominal Value	Perturbation Value Case 1	Perturbation Value Case 2	Unit
m_1	7.12	7.832	8.544	kg
m_2	6	5.4	4.8	kg
m_3	5.8	6.38	6.96	kg
k_1	9430	10373	11316	N/m
k_2	14100	12690	11280	N/m
k_3	0.1	0.09	0.08	N/m
c_1	0	0	0	Ns/m
c_2	0	0	0	Ns/m
c_3	70	63	56	Ns/m

can be further simplified to

$$F_{pc} = -[m_1\ddot{x}_1 + k_1(x_1 - x_2)] = \underbrace{9430(x_2 - x_1)}_{\text{A}} + \underbrace{(-7.12\ddot{x}_1)}_{\text{B}} \tag{7}$$

In order to find the main source of the fluctuation of PCCF, a PCCF waveform at the speed of 380km/h is given. As shown in Fig. 7, the main contribution of the fluctuation of the contact force is from B, but the impact of A shouldn't be ignored. Therefore, the purpose of reducing the fluctuation of PCCF can be achieved by minimizing the PCA and limiting the displacement difference between x_2 and x_1.

According to the above analysis, the multi-objective robust control strategy is proposed in this paper. It includes the following aspects:

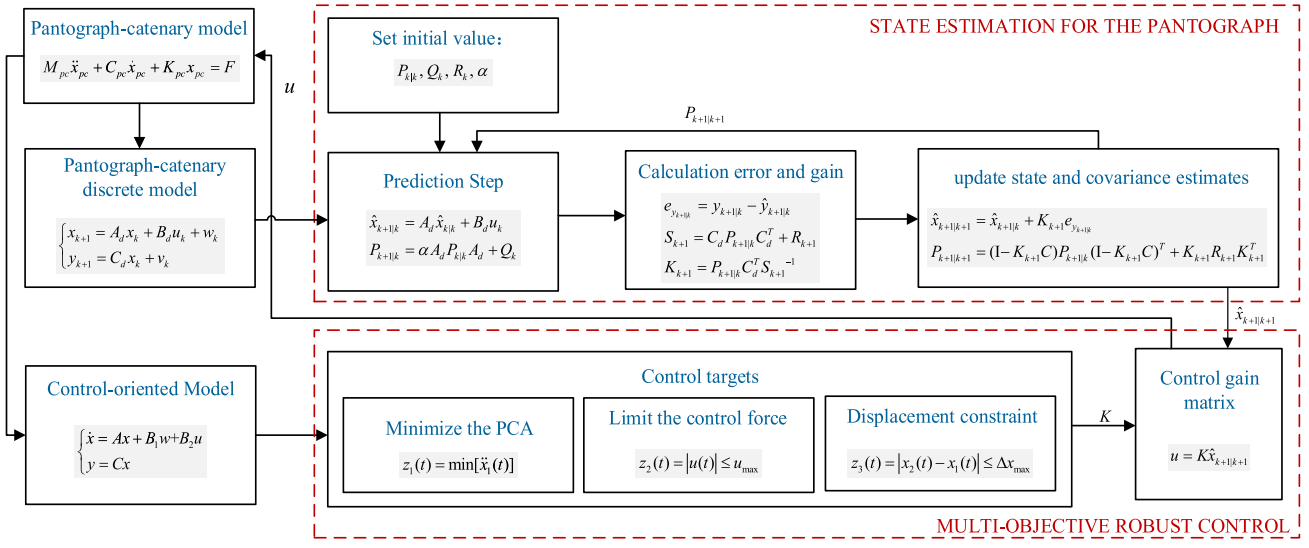

FIGURE 6. Schematic diagram of the proposed control strategy.

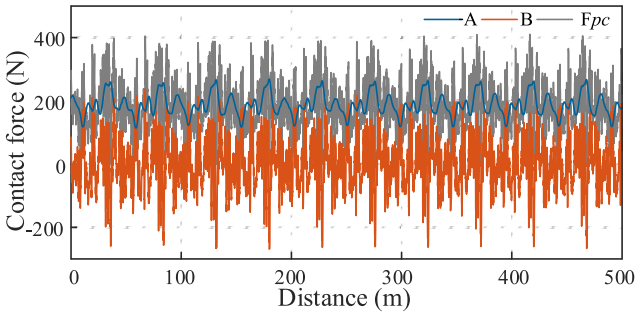

FIGURE 7. Influence of speed and displacement of pantograph on contact force.

1) **Minimize the PCA**: In order to reduce the fluctuation of PCCF, the vertical acceleration of the collector should be minimized.
2) **Limit the control force**: The energy of the active controller is limited, which means that the amplitude of the control force is bounded.
3) **Displacement constraint**: Avoid the negative impact on the displacement difference between x_2 and x_1 during the process of minimizing the PCA, so give it a constraint in advance. The constraint is to maintain the difference within the range of uncontrolled.

Based on the above considerations, the performance requirements (1)-(3) can be described as

$$\begin{cases} z_1(t) = \min[\ddot{x}_1(t)] \\ z_2(t) = |u(t)| \le u_{\max} \\ z_3(t) = |x_2(t) - x_1(t)| \le \Delta x_{\max} \end{cases} \tag{8}$$

where $z_1(t)$, $z_2(t)$ and $z_3(t)$ denote the controlled outputs of the multi-objective robust control system, $u_{\max}$ denotes the maximum control force, $\Delta x_{\max}$ denotes the maximum displacement difference between the first mass and the second mass.

In order to resign a control-oriented model, it is necessary to calculate the original static stiffness based on the nonlinear catenary model. The important point is able to represent the elasticity distribution along the contact wire. It is can be described as

$$k(t) = \sum_{i=1}^{8} a_i \exp\left(-\left(\frac{vt - b_i}{c_i}\right)^2\right) \tag{9}$$

where v and t denote the train speed and time, respectively. a_i, b_i and c_i are the fitting coefficients.

The contact force can be expressed as

$$F_{pc}(t) = k(t)x_1 \tag{10}$$

According to (1), (8) and (10), if the state variable is set as $\mathbf{x} = [x_1, \dot{x}_1, x_2, \dot{x}_2, x_3, \dot{x}_3]^T$, the corresponding state-space representation of PCS is given by

$$\begin{cases} \dot{\mathbf{x}}(t) = \mathbf{A}\mathbf{x}(t) + \mathbf{B}_1 w(t) + \mathbf{B}_2 u(t) \\ z_1(t) = \mathbf{C}_1\mathbf{x}(t) + B_{11}w(t) + B_{12}u(t) \\ z_2(t) = \mathbf{C}_2\mathbf{x}(t) + B_{21}w(t) + B_{22}u(t) \\ z_3(t) = \mathbf{C}_3\mathbf{x}(t) + B_{31}w(t) + B_{32}u(t) \end{cases} \tag{11}$$

where w represents the disturbance of the system, u denotes the active control force. The state matrix and the input matrix are as follows

$$\mathbf{A} = \begin{bmatrix} 0 & 1 & 0 & 0 & 0 & 0 \\ \frac{-(k_1+k(t))}{m_1} & \frac{-c_1}{m_1} & \frac{k_1}{m_1} & \frac{c_1}{m_1} & 0 & 0 \\ 0 & 0 & 0 & 1 & 0 & 0 \\ \frac{k_1}{m_2} & \frac{c_1}{m_2} & \frac{-(k_1+k_2)}{m_2} & \frac{-(c_1+c_2)}{m_2} & \frac{k_2}{m_2} & \frac{c_2}{m_2} \\ 0 & 0 & 0 & 0 & 0 & 1 \\ 0 & 0 & \frac{k_2}{m_3} & \frac{c_2}{m_3} & \frac{-(k_2+k_3)}{m_3} & \frac{-(c_2+c_3)}{m_3} \end{bmatrix},$$

$\mathbf{B}_1 = \begin{bmatrix} 0 & \frac{-1}{m_1} & 0 & 0 & 0 & 0 \end{bmatrix}^T$, $\mathbf{B}_2 = \begin{bmatrix} 0 & 0 & 0 & 0 & 0 & \frac{1}{m_3} \end{bmatrix}^T$, $B_{11} = -1/m_1 B_{22} = 1$, $\mathbf{C}_1 = \left[-(k_1 + k(t))/m_1, -c_1/m_1, k_1/m_1, c_1/m_1, 0, 0\right]$, $\mathbf{C}_2 = \mathbf{0}$, $\mathbf{C}_3 = \left[-1/\Delta x_{\max}, 0, 1/\Delta x_{\max}, 0, 0, 0\right]$, $B_{12} = B_{21} = B_{31} = B_{32} = 0$.

Therefore, the whole problem can be converted to design a state feedback law

$$u(t) = \mathbf{K}\mathbf{x}(t) \tag{12}$$

where K is the control gain matrix. The multi-objective robust control problem of the pantograph is to determine the control gain matrix meeting the following requirements:

- The closed-loop system is asymptotically stable.
- The control targets are guaranteed when the disturbance is not greater than $w_{\max}$.
- For all disturbances $w(t) \in L_2[0, \infty)$, the performance $||G_{z1}||_\infty < \gamma$ is guaranteed under zero initial condition. G_{z_1} denotes the transfer function from $w(t)$ to $z_1(t)$.

B. STATE ESTIMATION FOR THE PANTOGRAPH

It can be known from (11) and (12) that the calculation of the control force requires state variables of the pantograph. However, considering multiple sensors installed on a pantograph may reduce the reliability of control system, and the complex electromagnetic environment, the severe physical environment and other severe operating conditions can easily lead to inaccurate measurements. We assume that the observable quantity is the vertical displacement of each mass, and then estimates the vertical displacement and velocity of each mass. Therefore, an estimator is used to solve this problem. The discrete state space equation of the PCS can be described as

$$\begin{cases} \mathbf{x}_{k+1} = \mathbf{A}_d\mathbf{x}_k + \mathbf{B}_d u_k + \mathbf{w}_k \\ \mathbf{y}_{k+1} = \mathbf{C}_d\mathbf{x}_k + \mathbf{v}_k \end{cases} \tag{13}$$

where $\mathbf{A}_d, \mathbf{B}_d, \mathbf{C}_d$ are the correlation coefficient matrixes. $\mathbf{w}_k$ represents the process noise. $\mathbf{v}_k$ represents the measurement

noise, which are uncorrelated zero-mean Gauss white noise, and their covariance matrixes are $\mathbf{Q}_k$ and $\mathbf{R}_k$.

Therefore, the general Kalman filter estimation algorithm [22] is given as

$$\hat{\mathbf{x}}_{k+1|k} = \mathbf{A}_d\hat{\mathbf{x}}_{k|k} + \mathbf{B}_d u_k \tag{14}$$

$$\mathbf{P}_{k+1|k} = \mathbf{A}_d\mathbf{P}_{k|k}\mathbf{A}_d^T + \mathbf{Q}_k \tag{15}$$

$$\mathbf{K}_{k+1} = \mathbf{P}_{k+1|k}\mathbf{C}_d^T(\mathbf{C}_d\mathbf{P}_{k+1|k}\mathbf{C}_d^T + \mathbf{R}_k)^{-1} \tag{16}$$

$$\hat{\mathbf{x}}_{k+1|k+1} = \hat{\mathbf{x}}_{k+1|k} + \mathbf{K}_{k+1}(\mathbf{y}_{k+1|k} - \hat{\mathbf{y}}_{k+1|k}) \tag{17}$$

$$\mathbf{P}_{k+1|k+1} = \mathbf{P}_{k+1|k} - \mathbf{K}_{k+1}(\mathbf{C}_d\mathbf{P}_{k+1|k}\mathbf{C}_d^T + \mathbf{R}_k)\mathbf{K}_{k+1|k}^T \tag{18}$$

The Kalman filter is an effective algorithm for Gaussian process optimal filtering. When the object model is sufficiently accurate, the performance is better; but when the model has errors, this growth memory filter makes the ''old'' measurement data have an adverse effect on the current state estimation, and may even be scattered. This problem can be solved by the fading filter algorithm, which uses the forgetting factor to limit the memory length of the Kalman filter to make full use of the current measurement data. The filter estimation formulas are modified as follows

$$\mathbf{P}_{k+1|k} = \alpha\mathbf{A}_h\mathbf{P}_{k|k}\mathbf{A}_h^T + \mathbf{Q}_k \tag{19}$$

$$\mathbf{P}_{k+1|k+1} = (\mathbf{I} - \mathbf{K}_{k+1}\mathbf{C})\mathbf{P}_{k+1|k}(\mathbf{I} - \mathbf{K}_{k+1}\mathbf{C})^T + \mathbf{K}_{k+1}\mathbf{R}_{k+1}\mathbf{K}_{k+1}^T \tag{20}$$

The difference from the conventional Kalman filter is that the fading Kalman filter embodies the effect of the current measurement data on the state estimation.

C. MULTI-OBJECTIVE H_∞ CONTROLLER

Given positive scalars γ and ρ, if there are appropriate dimension matrix $\mathbf{P}>0$ that satisfying [26]–[28]

$$\begin{bmatrix} \bar{\mathbf{A}}\mathbf{P} + \mathbf{P}\bar{\mathbf{A}}^T & \bar{\mathbf{B}} & \mathbf{P}\bar{\mathbf{C}}^T \\ * & -\mathbf{I} & \bar{\mathbf{D}}^T \\ * & * & -\gamma^2\mathbf{I} \end{bmatrix} < 0 \tag{21}$$

$$\begin{bmatrix} 1 & \sqrt{\rho}\mathbf{K}\mathbf{P} \\ * & -u_{\max}^2\mathbf{P} \end{bmatrix} < 0 \tag{22}$$

$$\begin{bmatrix} 1 & \sqrt{\rho}\mathbf{C}_2\mathbf{P} \\ * & -\mathbf{P} \end{bmatrix} < 0 \tag{23}$$

with $\begin{bmatrix} \bar{\mathbf{A}} & \bar{\mathbf{B}} \\ \bar{\mathbf{C}} & \bar{\mathbf{D}} \end{bmatrix} = \begin{bmatrix} \mathbf{A} + \mathbf{B}_2\mathbf{K} & \mathbf{B}_1 \\ \mathbf{C}_1 + \mathbf{B}_{12}\mathbf{K} & \mathbf{B}_{12} \end{bmatrix}$, where ''$*$'' denotes transposed matrix of symmetry position. If the above matrix inequality group has a solution, the value of K in the inequality can be obtained.

Then, combining the estimator results, the optimal active control force can be described as

$$u(k) = \hat{\mathbf{K}}\mathbf{x}(k) \tag{24}$$

IV. SIMULATION STUDY

With different work conditions, several cases are given to verify the effectiveness and robustness of the proposed control strategies. In these cases, the real physical parameters of DSA380 pantograph and the catenary of Beijing-Tianjin high-speed network are adopted as shown in Table 1 and Table 2.

TABLE 2. Main parameters of catenary of Beijing-Tianjin high-speed line.

Parameter	Value	Unit
Span	48	m
Stagger	±200	mm
Contact wire tension	27	kN
Contact wire density	1.083	kg/m
Mess. wire tension	21	kN
Mess. wire density	1.068	kg/m
Number of droppers	5	/
Encumbrance	1.6	m
Pre-sag	5‰	/
Interval between droppers	5 m/9.5 m/9.5 m/9.5 m/9.5 m/5 m	

A. PERFORMANCE OF THE ESTIMATOR FOR PANTOGRAPH

This case investigates the performance of the estimator implemented in a nominal pantograph-catenary model. This paper assumes that the observable quantity is the vertical displacement of each mass, and then estimates the vertical displacement and velocity of each mass. The main initial values of the estimator are set as $v = 360$km/h, $Q = 10^{-8}\ eye(6)$, $R = diag[10^{-4}, 10^{-4}, 10^{-4}]$, $\hat{x}_{0|0} = zeros(6, 1)$, $P_{0|0} = 10^{-6}\ eye(6)$ and $\alpha = 1.01$. Fig. 8 (a)-(c) denotes the measured, actual and estimated values of the vertical displacements of the masses 1, 2 and 3, respectively, Fig. 8 (d)-(f) show the actual and estimated values of the vertical speed of the pantograph mass, respectively. The values of root mean square errors with respective to Figure 6 are 0.0006, 0.0006, 0.0006, 0.0186, 0.0346 and 0.0268, respectively, which can be totally neglected. Therefore, the estimation algorithm can estimate the states with high efficiency.

B. INVESTIGATION OF THE PERFORMANCE OF CONTROLLER

The effectiveness and robustness of the controller is verified with a nonlinear PCS model. The control gain matrix is calculated according to the parameters in Table 1 and Table 2 as: $K = 10^3 * [-3.3868\ 0.0736\ 4.7303\ 0.0016\ -3.2227\ -0.1139]$ Then, the performance of the control strategy is evaluated with the nonlinear PCS model. The PCCFs at the speed of 280km/h, 320km/h and 360km/h are shown in Fig. 9 (a)-(c), respectively. The PCA under different operational speeds are shown in Figure 9 (d)-(f). The standard deviation (STD) of the PCCF are decreased by 29.55%, 25.26% and 20.86% and the STD of the PCA are decreased by 23.20%, 15.20% and 12.60%, respectively. With the increase of the train speed, the performance of the controller is gradually reduced, but the fluctuation of the PCCF can still be

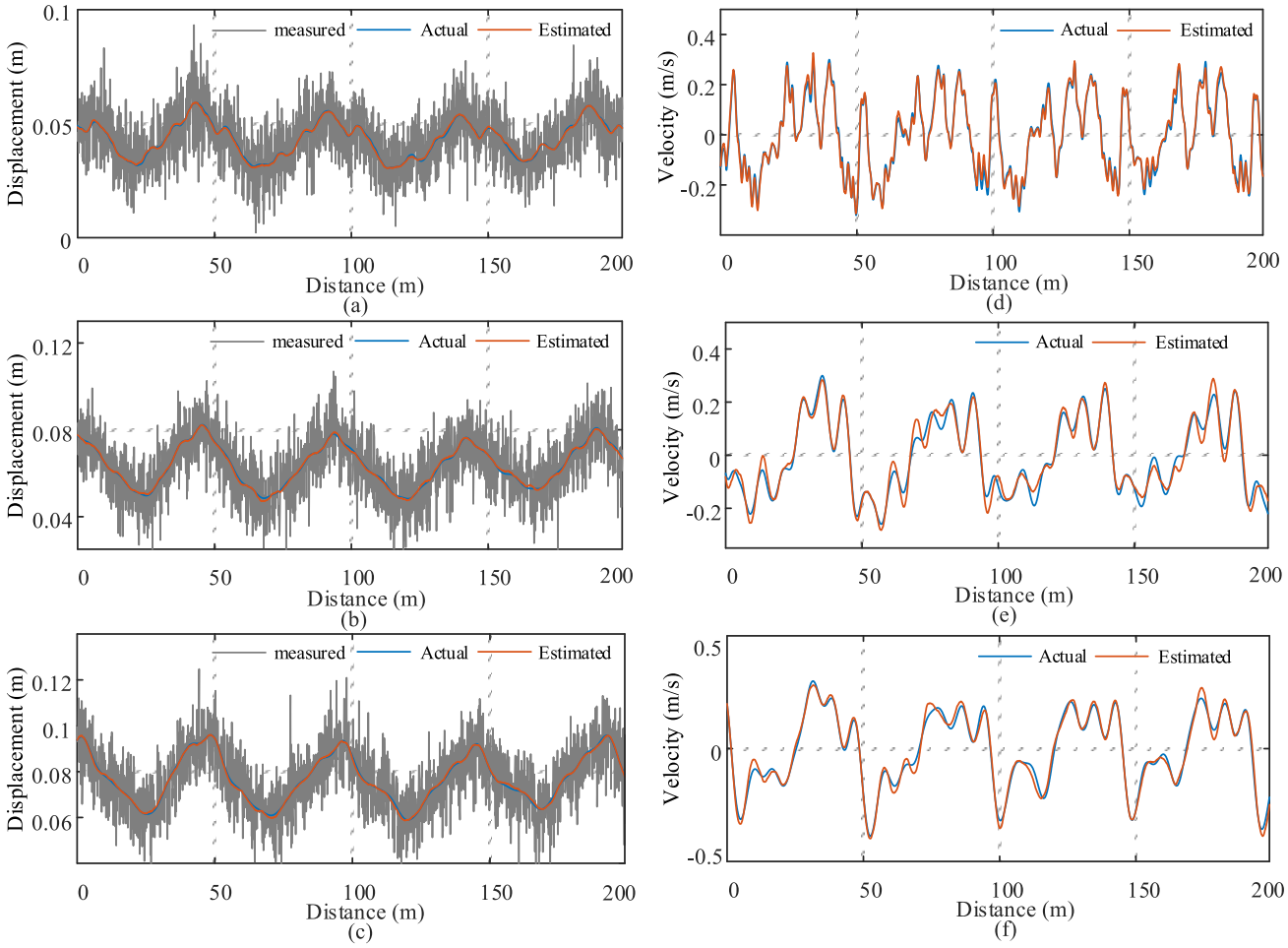

FIGURE 8. Measured states, estimated states and actual states of the pantograph. (a)-(c) displacements of mass 1 - mass 3; (d)-(f) velocities of mass 1 - mass 3.

effectively reduced. Compared to the control strategy in [24], the proposed control performance is better.

The fluctuation of the contact force (reflected by the STD of PCCF) is reduced, but it is not sufficient to explain the pros and cons of the controller. In general, the controller needs to maintain the average value of the contact force while reducing the fluctuation of PCCF. Comparing the simulation results of different work conditions, the bar of PCCF and PCA as shown in Fig. 10, which 'No_280' and 'CL_280' respectively represent the results without control, with control at 280 km/h; in the same way, 'No_320' and 'CL_320' denote the uncontrolled and controlled results at 320 km/h, respectively. It can be seen from Fig. 10 that the maximum value of the PCCF and PCA are decreased, the minimum values are increased, and the mean value remains unchanged.

As can be seen from (24), the characteristics of the control force depend on the gain matrix 'K' and the pantograph state variable 'x'. The value of the gain matrix K is constant during the control process, and the displacement and velocity of each mass of the pantograph has a low frequency (it can be seen from Fig. 8). Therefore, the control force has a low frequency as show in Fig. 11, and its dominant frequency is around 2Hz. In addition, the comparison of the control forces with [24] is shown in Figure 12, the amplitude of the control force is significantly smaller. In other words, the result of proposed control strategy is better than the control result in [24], even though the proposed controller requires a lower energy consumption.

The time from the acquisition of state information to the active control force acting on the PCS is called the actuator time delay. The time delay problem and its impact will occur when actuator needs to move. Therefore, when the actuator does not need to operate, the time delay problem naturally does not need to be considered. This paper attempts to reduce the negative effects of time delay by reducing the number of actuator actions, rather than eliminate the actuator's time-delay. According to the low frequency characteristics of the active control force, the active control force can be pre-processed to reduce the number of actuator actions.

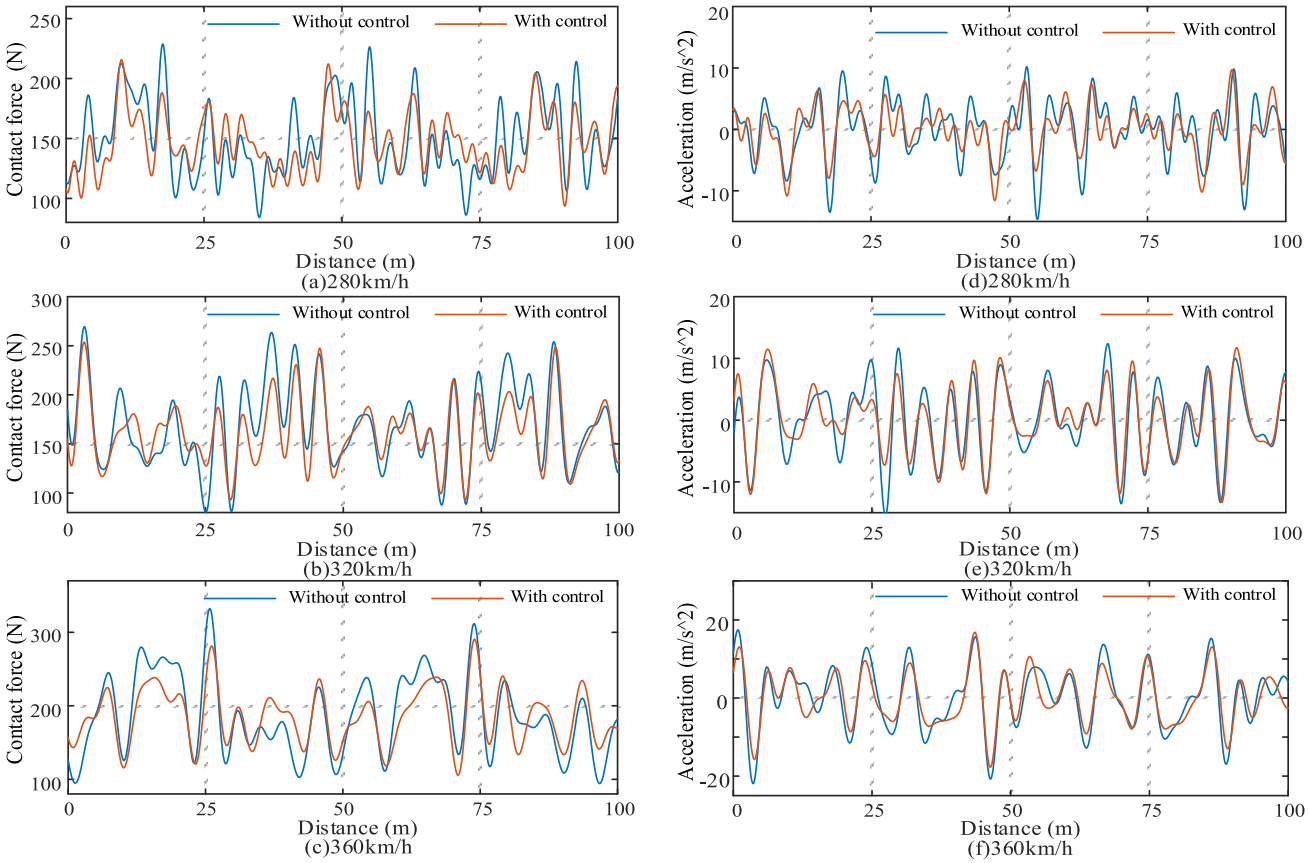

FIGURE 9. Comparison of the contact force and its acceleration under different speeds.

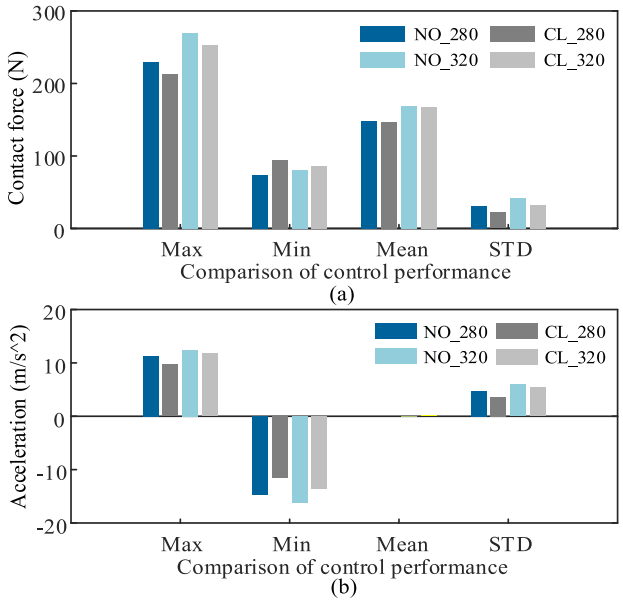

FIGURE 10. Histograms of contact force and collector acceleration at 280km/h and 320km/h.

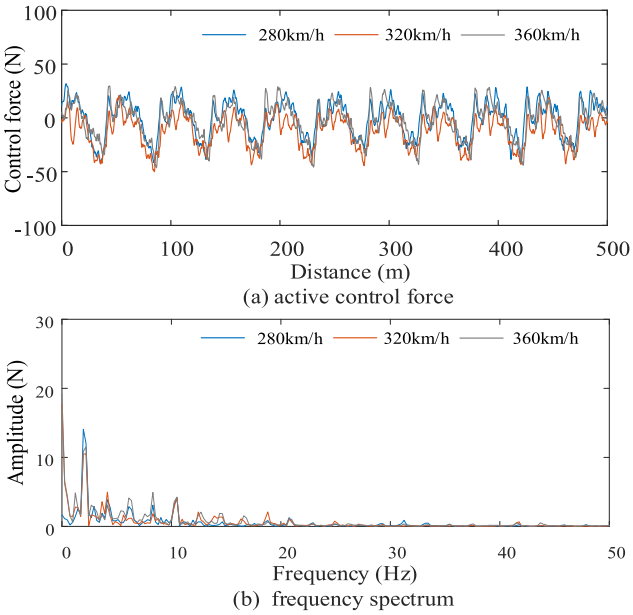

FIGURE 11. Active control force and its spectrum under different operational speed.

The processing method is as follows

$$u^*(t) = \begin{cases} u_h & u(t) > u_s \\ u_l & u(t) \le u_s \end{cases} \tag{25}$$

where $u^*(t)$ denotes control force after being processed, $u_h(t)$, $u_l(t)$ and u_s all represent positive constants, which can be obtained from the control force before pre-processing.

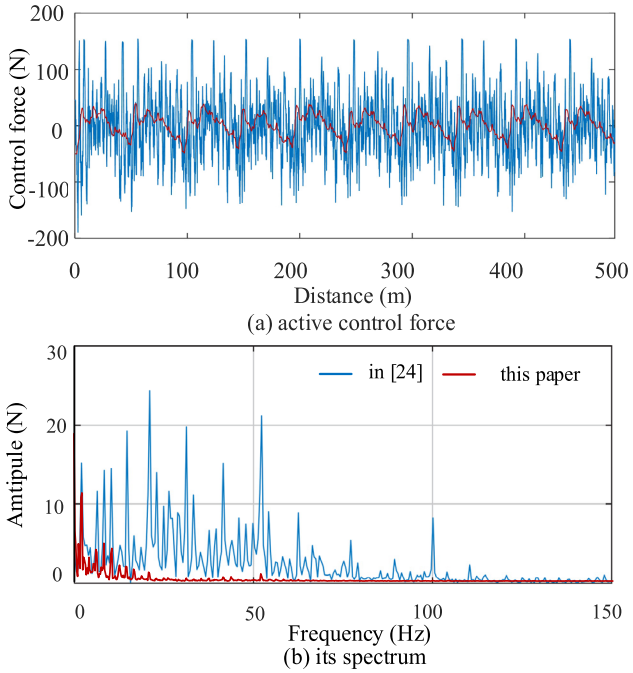

FIGURE 12. Control force and its spectrum under different control strategies at 360 km/h.

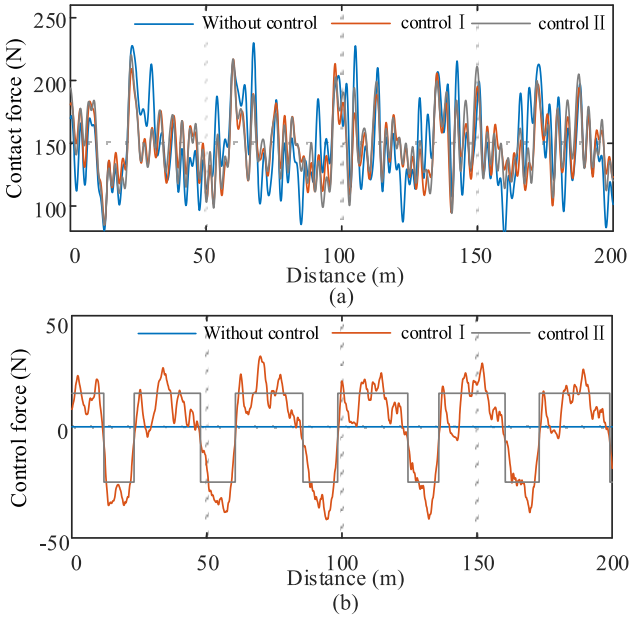

FIGURE 13. Contact force under different control laws at 280km/h.

The simplified control force is shown in Fig. 13(b), which 'control I' is the control force before unprocessed and 'control II' is the control force after processing. The contact force as shown in Fig. 13(a). After the active control force is preprocessed, the STD of the PCCF is decreased by 24.46%. In this case, the optimality of the controller is lost, but the number of actuator actions is significantly reduced.

The time delay is a characteristic of the actuator itself. In Fig. 13, the running speed of the high-speed train

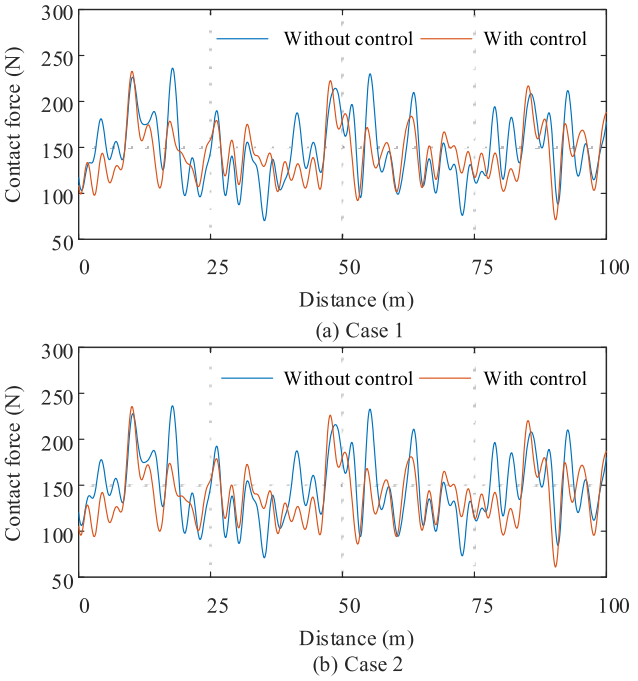

FIGURE 14. Contact force at 280m/h under the parameter perturbation of the pantograph.

is 280km/h, so it can be estimated that the maximum actuation time interval in the controller II is 0.321 seconds. When the time delay of actuator is less than the maximum actuation time interval in controller II, the designed controller provides a solution for reduce the impact of the actuator time delay. In summary, the time delay acceptable for the controller designed should be less than the maximum actuation time interval.

C. ROBUSTNESS INVESTIGATION FOR PARAMETER UNCERTAINTIES OF PANTOGRAPHS

The above simulations are performed under ideal conditions without considering parameter perturbation. In fact, there is always a slight error between the ideal model and the actual system. In this section, the control performance is evaluated with the parameter perturbation of the pantograph. The parameters are intentionally changed, as shown in Table 1. The calculated results for different cases are shown in Fig. 14. The STD of the contact force is reduced by 20.35% and 18.37% from the simulation results, respectively. It is worth noting that the parameter perturbation of the pantograph is almost less than the value of case 1 or case 2. Therefore, the control strategy proposed in this paper can deal with the parameter perturbation of the pantograph efficiently.

D. ROBUSTNESS INVESTIGATION FOR THE UNEVENNESS OF CONTACT LINES

The unevenness of contact lines is one of the factors that considerably influences the dynamic characteristics of current collection systems. In electrified railways, the unevenness of

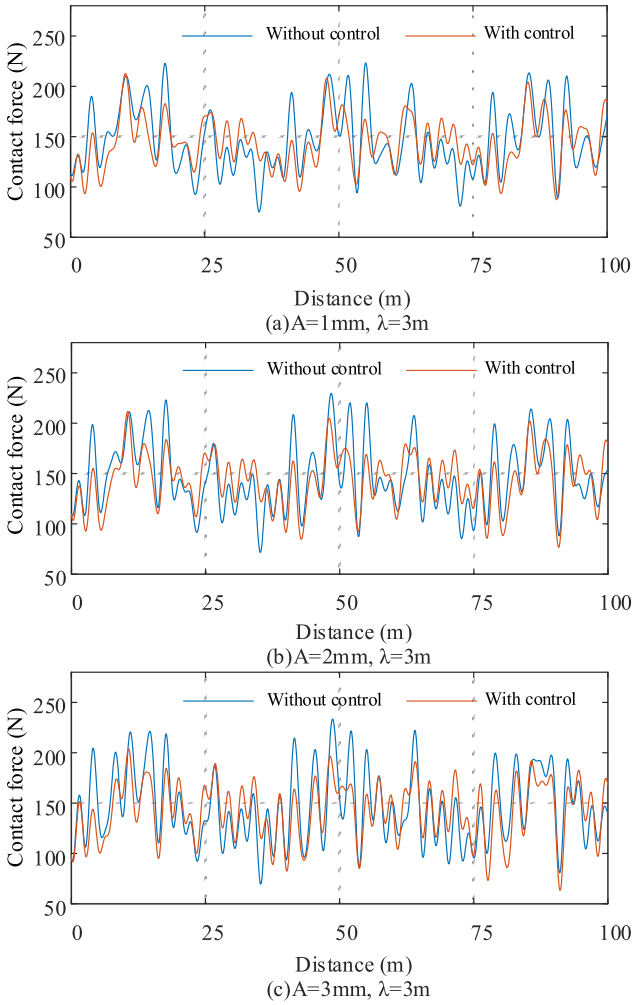

FIGURE 15. Contact force with the unevenness of contact lines under operation speed 280 km/h.

the contact line is determined by the position and shape of the contact line itself and the wear of the contact line surface. In the finite element model of the catenary, the equation of the unevenness of contact lines [29] can be described as

$$y(x) = \frac{1}{2}A\left[1 - \cos\left(\frac{2\pi x}{\lambda}\right)\right] \tag{26}$$

where A represents the uneven amplitude, λ denotes the uneven wavelength, and x represents the coordinate along the contact line. According to the previous research work [29]–[31], the robustness of the proposed control strategy for the unevenness of contact lines is investigated. Fig. 15 shows the contact force with and without control under the unevenness of contact lines. It can be seen that the control strategy performs well, even though the fluctuation in contact force is greatly aggravated by the unevenness of contact lines. In Fig. 15(a)–(c), the STD of contact force is reduced by 29.13%, 24.17% and 16.94% respectively. Therefore, the proposed control strategy has a good robustness to reject external disturbance. In addition, as the unevenness of contact lines increases, the performance of the controller gradually decreases.

V. CONCLUSION

In this paper, a controller is proposed for the active pantograph to reduce the fluctuation of PCCF. The model of pantograph-catenary interaction is established based on the finite element approach and the multibody dynamics. A Kalman filter is designed to obtain the states of the pantograph considering complex electromagnetic circumstances and severe physical environments. The factors causing the fluctuation of the contact force are analyzed to determine the three control targets, which are minimize the PCA, limit the control force and displacement constraint. At last, a multi-objective robust control method based on state estimation is designed, and the effectiveness and robustness of the proposed control strategy are verified with the nonlinear PCS model. The conclusions are drawn as follows

(1) For the pantograph state estimation, the errors of the vertical displacement and velocity of the pantograph masses are 0.0006, 0.0006, 0.0006, 0.0186, 0.0346, and 0.0268, respectively.
(2) When the operational speeds of high-speed trains are 280km/h, 320km/h and 360km/h, the STD of PCCF is reduced by 29.55%, 25.26% and 20.86%, respectively. The STD of PCA is respectively reduced by 23.20%, 15.20% and 12.60%.
(3) Compared with the previous pantograph control strategy, the result of proposed control strategy is better than the control result in [24], even though the proposed controller requires a lower energy consumption.
(4) Due to the low frequency characteristics of the active control force, this paper attempts to reduce the negative effects of time delay by reducing the number of actuator actions. In addition, after the pre-treatment of the active control force, the number of actuator actions is reduced, and the control is still effective.
(5) With the parameter disturbance of pantograph, the STD of PCCF is still reduced by 20.35% and 18.37% at 280km/h. In other words, the control strategy proposed in this paper can deal with the parameter perturbation of the pantograph efficiently. In addition, as the unevenness of contact lines increases, the performance of the controller gradually decreases.

In the future, considering the limitations of numerical simulation, the interaction between the physical pantograph and the catenary is not perfectly reflected [32]. Therefore, more research will be based on a hybrid simulation of pantograph-catenary interactions. It is worthwhile to note that the pantograph is considered as the lumped-mass model in this paper, which may be not realistic. And, the measurement accuracy of the state variables of the pantograph and the high-voltage electromagnetic interference are not considered [33], which may trigger some changes in calculation control force. In the future, these factors will be taken into account and the active

control for high-speed railway pantograph-catenary will be investigated extensively.

REFERENCES

[1] J. H. Lee, T. W. Park, H. K. Oh, and Y. G. Kim, "Analysis of dynamic interaction between catenary and pantograph with experimental verification and performance evaluation in new high-speed line," *Vehicle Syst. Dyn.*, vol. 53, no. 8, pp. 1117–1134, 2015.

[2] B. Allotta, L. Pugi, and F. Bartolini, "Design and experimental results of an active suspension system for a high-speed pantograph," *IEEE/ASME Trans. Mechatronics*, vol. 13, no. 5, pp. 548–557, Oct. 2008.

[3] J. Ambrósio, J. Pombo, and M. Pereira, "Optimization of high-speed railway pantographs for improving pantograph-catenary contact," *Theor. Appl. Mech. Lett.*, vol. 3, no. 1, Jan. 2013, Art. no. 013006.

[4] J. Pombo and J. Ambrósio, "Influence of pantograph suspension characteristics on the contact quality with the catenary for high speed trains," *Comput. Struct.*, vols. 110–111, pp. 32–42, Nov. 2012.

[5] X. Li, D. Zhou, L. Jia, and M. Yang, "Effects of yaw angle on the unsteady aerodynamic performance of the pantograph of a high-speed train under crosswind," *J. Wind Eng. Ind. Aerodyn.*, vol. 182, pp. 49–60, Nov. 2018.

[6] L. Chen, P. Peng, and F. He, "Fatigue life analysis of dropper used in pantograph-catenary system of high-speed railway," *Adv. Mech. Eng.*, vol. 10, no. 5, May 2018, Art. no. 1687814018776135.

[7] W. Zhang, N. Zhou, R. Li, G. Mei, and D . Song, "Pantograph and catenary system with double pantographs for high-speed trains at 350 km/h or higher," *J. Mod. Transp.*, vol. 19, no. 1, pp. 7–11, Mar. 2011.

[8] Y. Song, Z. Liu, H. Wang, J. Zhang, X. Lu, and F. Duan, "Analysis of the galloping behaviour of an electrified railway overhead contact line using the non-linear finite element method," *Proc. Inst. Mech. Eng., F, J. Rail Rapid Transit*, vol. 232, no. 10, pp. 2339–2352, Apr. 2018.

[9] W. Zhou, H. T. Xiao, Z. G. Wang, L. Chen, and S. Q. Fu, "Dynamic target template matching for railway catenary suspension motion detection in wind area," *Int. J. Distrib. Sensor Netw.*, vol. 14, no. 9, Sep. 2018, Art. no. 1550147718797956.

[10] P. Zdziebko, A. Martowicz, and T. Uhl, "An investigation on the active control strategy for a high-speed pantograph using co-simulations," *Proc. Inst. Mech. Eng., I, J. Syst. Control Eng.*, vol. 233, no. 4, pp. 370–383, Jun. 2019.

[11] Y. Song, H. Ouyang, Z. Liu, G. Mei, H. Wang, and X. Lu, "Active control of contact force for high-speed railway pantograph-catenary based on multi-body pantograph model," *Mech. Mach. Theory.*, vol. 115, pp. 35–59, Sep. 2017.

[12] C. Sanchez-Rebollo, J. R. Jimenez-Octavio, and A. Carnicero, "Active control strategy on a catenary–pantograph validated model," *Vehicle Syst. Dyn.*, vol. 51, no. 4, pp. 554–569, Feb. 2013.

[13] T.-C. Lin, J.-L. Yeh, C.-H. Kuo, Y.-C. Lin, and V. E. Balas, "Adaptive fuzzy sliding mode active vibration control for rail vehicle pantograph," in *Proc. IEEE Int. Conf. Fuzzy Syst.*, Jul. 2016, pp. 373–379.

[14] Y. Song, Z. G. Liu, H. Ouyang, H. R. Wang, and X. B. Lu, "Sliding mode control with pd sliding surface for high-speed railway pantograph-catenary contact force under strong stochastic wind field," *Shock Vib.*, vol. 2017, Jan. 2017, Art. no. 4895321.

[15] A. Pisano and E. Usai, "Contact force estimation and regulation in active pantographs: An algebraic observability approach," in *Proc. IEEE Conf. Decis. Control.*, Dec. 2007, pp. 4341–4346.

[16] Y.-C. Lin, N.-C. Shieh, and V.-T. Liu, "Optimal control for rail vehicle pantograph systems with actuator delays," *IET Control Theory Appl.*, vol. 9, no. 13, pp. 1917–1926, Aug. 2015.

[17] Y.-C. Lin, C.-L. Lin, and C.-C. Yang, "Robust active vibration control for rail vehicle pantograph," *IEEE Trans. Veh. Technol.*, vol. 56, no. 4, pp. 1994–2004, Jul. 2007.

[18] Z. Liu, Y. C. Liu, N. Zhou, D. Zou, and H. Y. Tu, "Backstepping controller design for pantograph-catenary system," *IOP Conf., Mater. Sci. Eng.*, vol. 428, no. 1, Sep. 2018, Art. no. 012045.

[19] Y. Wu, J. H. Zheng, and T. Q. Zheng, "Optimizing active control scheme of high-speed pantograph," in *Proc. IEEE 6th Int. Power Electron. Motion Control Conf.*, May 2009, pp. 2622–2626.

[20] A. N. Vargas, H. M. T. Menegaz, J. Y. Ishihara, and L. Acho, "Unscented Kalman filters for estimating the position of an automotive electronic throttle valve," *IEEE Trans. Veh. Technol.*, vol. 65, no. 6, pp. 4627–4632, Jun. 2016.

[21] J.-C. Juang and C.-F. Lin , "A sensor fusion scheme for the estimation of vehicular speed and heading angle," *IEEE Trans. Veh. Technol.*, vol. 64, no. 7, pp. 2773–2782, Jul. 2015.

[22] H. H. Afshari, S. A. Gadsden, and S. Habibi, "Gaussian filters for parameter and state estimation: A general review of theory and recent trends," *Signal Process.*, vol. 135, pp. 218–238, Jun. 2017.

[23] Y. Yamashita and S. Kobayashi, "Method to improve adaptation speed of control parameters for active control pantographs," *Quart. Rep. RTRI*, vol. 57, no. 4, pp. 305–310, Nov. 2016.

[24] X. B. Lu, Z. G. Liu, Y. Song, H. R. Wang, J. Zhang, and Y. B. Wang, "Estimator-based multiobjective robust control strategy for an active pantograph in high-speed railways," *Proc. Inst. Mech. Eng., F, J. Rai Rapid Transit*, vol. 232, no. 4, pp. 1064–1077, Apr. 2018.

[25] X. Lu, Z. Liu, J. Zhang, H. Wang, Y. Song, and F. Duan, "Prior-information-based finite-frequency H_∞ control for active double pantograph in high-speed railway," *IEEE Trans. Veh. Technol.*, vol. 66, no. 10, pp. 8723–8733, Oct. 2017.

[26] G. Wang, C. Chen, and S. B. Yu, "Robust non-fragile finite-frequency H_∞ static output-feedback control for active suspension systems," *Mech. Syst. Signal Process.*, vol. 91, pp. 41–56, Jul. 2017.

[27] H. Chen, P.-Y. Sun, and K.-H. Guo, "Constrained H-infinity control of active suspensions: An LMI approach," in *Proc. Int. Conf. Control Autom. ICCA Final Prog. Book Abstr.*, Jun. 2002, p. 157.

[28] Y. Zhao, W. Sun, and H. Gao, "Robust control synthesis for seat suspension systems with actuator saturation and time-varying input delay," *J. Sound Vib.*, vol. 329, no. 21, pp. 4335–4353, Oct. 2010.

[29] W. H. Zhang, G. M. Mei, and L. Q. Chen, "Analysis of the influence of catenary's sag and irregularity upon the quality of current-feeding," *J. China Railway Soc.*, vol. 22, no. 6, pp. 50–54, Dec. 2000.

[30] M. Aboshi, "Precise measurement and estimation method for overhead contact line unevenness," *Elect. Eng. Jpn.*, vol. 160, no. 2, pp. 77–85, Jul. 2010.

[31] R.-H. Zhai, J.-H. Jiao, G.-H. Su, T.-F. Liu, and W.-Q. Zhu, "Dynamics of pantograph-catenary coupled system with contact wire vertical irregularities," *J. China Railway Soc.*, vol. 34, no. 7, pp. 24–29, Jul. 2012.

[32] A. Facchinetti and M. Mauri, "Hardware-in-the-loop overhead line emulator for active pantograph testing," *IEEE Trans. Ind. Electron.*, vol. 56, no. 10, pp. 4071–4078, Oct. 2009.

[33] S. Bruni, G. Bucca, M. Carnevale, A. Collina, and A. Facchinetti, "Pantograph–catenary interaction: Recent achievements and future research challenges," *Int. J. Rail Transp.*, vol. 6, pp. 57–82, Nov. 2017.

JING ZHANG received the Ph.D. degree in mechanical manufacturing engineering and automation from Southwest Jiaotong University, Sichuan, China, in 2008. She is currently an Associate Professor with the School of Electrical Engineering, Southwest Jiaotong University. Her current research interests include optimization design of pantograph-catenary parameters, aerodynamics of pantograph-catenary system, and control technology of high-speed pantograph.

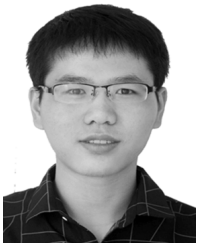

HANTAO ZHANG received the bachelor's degree in electrical engineering from East China Jiaotong University, Nanchang, China. He is currently pursuing the master's degree in electrical engineering with Southwest Jiaotong University, Chengdu, China. His research interests include the pantograph-catenary system modeling and active control of pantograph.

BAOLIN SONG received the bachelor's degree in electrical engineering from the Chengdu University of Technology, Chengdu, China. He is currently pursuing the master's degree in electrical engineering with Southwest Jiaotong University, Chengdu. His research interests include pantograph-catenary dynamics model, state observation, and pantograph active control method.

SONGLIN XIE received the bachelor's degree in electrical engineering from Southwest Jiaotong University, Chengdu, China, where he is currently pursuing the master's degree. His research interests include active control of pantograph.

ZHIGANG LIU (M'06–SM'16) received the Ph.D. degree in power system and automation from Southwest Jiaotong University, Chengdu, China, in 2003. He is currently a Full Professor with the School of Electrical Engineering, Southwest Jiaotong University. His current research interests include electrical relationship of vehicle-grid in high-speed railways, power quality considering grid-connect of new energies, pantograph-catenary dynamics, fault detection, status assessment, and active control. He was elected as a Fellow of the Institution of Engineering and Technology (IET), in 2017. He is currently an Associate Editor of the IEEE TRANSACTIONS ON INSTRUMENTATION AND MEASUREMENT, the IEEE TRANSACTIONS ON VEHICULAR TECHNOLOGY, and IEEE ACCESS.